AUTHOR'S POST PRINT (Romeo Colour: Green)
Int. J. of Heat and Mass Transfer (ISSN: 0017-9310), 47 (3): 601-612 (2004).
DOI:10.1016/S0017-9310(03)00337-5
Publisher version available at
http://www.sciencedirect.com/science/article/pii/S0017931003003375

Dissolution and solutal convection in partially miscibile liquid systems

Raffaele Savino*, Marcello Lappa°

(*) Università degli Studi di Napoli "Federico II"
Dipartimento di Scienza e Ingegneria dello Spazio "Luigi G. Napolitano"
P.le V.Tecchio 80, 80125 Napoli (Italy)

(°) MARS Center
(Microgravity Advanced Research and Support Center)
Via Emanuele Gianturco 31, 80142 Napoli (Italy)
Current e-mail address: marcello.lappa@strath.ac.uk

Abstract

A numerical model is developed to study the dissolution of droplets in a binary mixture with miscibility gap. The moving boundary problem is solved with a modified volume of fraction method to compute the time evolution of the average drop radius and the velocity and concentration distributions around the dissolving drop. The modeling results are presented to explain experimental findings that show stable and oscillatory plumes rising from droplets of methanol that dissolve into a cyclohexane liquid matrix.

INTRODUCTION

In recent years binary liquid-liquid systems, and particularly partially miscible liquid pairs, have been finding increasing applications in fundamental studies of interphase mass transfer. For instance, transparent liquids are often used as models for the investigation of the behaviour of opaque metal alloys in the liquid state .

Typically these alloys are solidified through phase diagrams that exhibit a miscibility gap [1]. The two-phase liquid consists of dispersed drops in a matrix liquid; the quality of the dispersion alloys is defined by the degree of homogeneity of the minority phase distribution since the strength of the metal alloys can be improved by a uniform dispersion of fine particles in the matrix. During alloy solidification, the melt is subject to temperature and concentration gradients that, in a gravity field, lead in most cases to buoyancy driven convective flows. Moreover, as the concentration of elements is different in both phases, the minority phase may experience buoyancy or sedimentation (Prinz and Romero [2]).

Due to the major difficulty in investigating liquid metals for their opaqueness, organic liquids are often used as model substances to study the flow and the solidification of alloys. For instance, Methanol and Cyclohexane have been selected and investigated both in Earth and in Space laboratories since they are transparent liquids exhibiting a miscibility gap in the phase diagram; in addition, the small difference in density (0.769 [g/cm^3] the Cyclohexane, 0.782 [g/cm^3] the Methanol) allows one, in principle, to minimize buoyancy and sedimenation effects.

One basic problem to be studied to some extent is the migration of drops in a fluid subject to a temperature gradient, in a gravity field as well as under microgravity conditions (see e.g. [3]). Furthermore, the issues of coalescence, growth and disappearance of drops during the phase separation process are of basic importance.

In preparation of a microgravity experiment to be performed on board a sounding rocket to study the dissolution and Marangoni migration of methanol drops in a non isothermal liquid matrix of Cyclohexane, the droplet dissolution under normal gravity conditions has been investigated.

A droplet of Methanol was formed on the tip of a capillary immersed into the Cyclohexane to study the droplet dissolution. The experimental procedure involved visual observation of the drop using a Wollastone optical apparatus to study the mass transfer at the binary liquid-liquid interface.

In spite of the small differences in density between the drop and the surrounding matrix, a convective plume was clearly observed; the plume, originated at the tip of the drop and directed upward, exhibits in some case pronounced regular oscillations that reveal a convective instability of the oscillatory type.

In previous experiments with different liquid-liquid systems (Aniline/Water, Isobutanol/Water, Ethilacetate/Water, see Agble and Mendes Tatsis [4]) a similar convective plume was observed that sometimes became unstable due to Marangoni effects induced by surfactants. In the above mentioned studies, the systems basically consisted of sitting drops (if the drop liquid is lighter than that of the matrix) or of pendant drops (if the drop liquid is heavier than that of the matrix). Correspondingly, the convective plume is directed downward (for pendant drop) or upward (for sitting drop). In the system under investigation, the droplet (Methanol) is heavier than the surrounding matrix but unexpectedly a rising convective plume is observed at the dissolving liquid-liquid interface.

The purpose of the present paper is to provide a theoretical explanation of the observed phenomena and to develop a numerical model for an adequate description of the system behaviour.

In addition, computations are carried out to show the ability of the numerical model to study the dissolution or growth of droplets of the minority phase in the miscibility gap of the phase diagram.

EXPERIMENTS

The experiments were performed with a Wollaston interferometer, using a Hellma cell made of quartz, 1 [cm] x 1 [cm] x 4 [cm], filled with liquid. The droplet of a liquid partially miscible with that of the matrix (volume ranging from 1 to 5 [μl]) was formed at the tip of a capillary (1mm

diameter). The temperature of the system is uniform and controlled by Peltier elements at the top and bottom walls. The drop liquid will be denoted as phase 1 and the liquid matrix as phase 2.

Figure 2 shows an image of a droplet of Buthanol dissolving in water. Since Buthanol is lighter than water (ρ_1=0.81 [g/cm^3] ; ρ_2= 1 [g/cm^3]) a convective plume originates at the dissolving interface directed upward.

Figure 3 shows the behaviour of a droplet of Methanol in a matrix of Hexane. In this case the drop liquid is heavier than the liquid matrix (ρ_1=0.782 [g/cm^3] ; ρ_2=0.65 [g/cm^3]) so that the flow around the dissolving droplet is directed downward.

Figure 4 shows a dissolving drop of Methanol in Cyclohexane. As explained before, Methanol is heavier than Cyclohexane (ρ_1=0.782 [g/cm^3]; ρ_2= 0.769 [g/cm^3]) so that one should expect a behaviour similar to that of Figure 3. On the contrary, a convective plume originates at the dissolving interface directed upward, similar to the case of Figure 2.

This phenomenon can be explained by the density dependence as function of the concentration for the Cyclohexane-Methanol system. According to the literature (Ref. [5]), the density of the Cyclohexane-Methanol binary mixture can be a decreasing or an increasing function of the methanol concentration depending on the concentration range. The density is a decreasing function of the methanol concentration for $0<c<c_1$, whereas it is an increasing function of c for $c_2<c<1$ ((c_1 and c_1 are the methanol concentrations at the consolute points of the miscibility diagram, see Figure 5). When a drop of pure Methanol is injected into the Cyclohexane liquid matrix, equilibrium at the liquid-liquid interface is attained instantaneously (Perez De Ortiz and Sawistowski [6]). Assuming negligible thermal effects (temperature differences less than 0.2 [°C] were measured with thermocouples), according to the phase rule the concentrations at the interface will be c_1 and c_2 (outside and inside the droplet, respectively, see Figure 5). Correspondingly the mixture surrounding the droplet is lighter than the external matrix and therefore a rising plume is originated.

The time evolution of the average droplet radius was measured for different values of the initial volume and different temperatures. Typical results obtained at ambient temperature are shown in Figure 6, for the case of a droplet with initial volume of 3 [μl].

The experiments have shown that when the initial volume of the droplet exceeds a critical value, depending on the experimental conditions (e.g. the temperature), after a transient time, depending on the temperature and on the initial volume, the plume exhibits periodic oscillations that reveal a convective instability (Figure 7). During the experiments instability was found, at ambient temperature, when the initial volume of the droplet was larger than 3 [μl], and that the period of the oscillations is an increasing function of the droplet diameter.

These results will be presented in a forthcoming paper dedicated to the detailed analysis of the experimental findings.

NUMERICAL MODEL

Basic assumptions

Fig.1 shows the geometry of the problem and the boundary conditions. A liquid drop is suspended in a liquid matrix. The liquid system (drop and matrix) is in a region of the phase diagram (T versus C) where it separates continuously into two phases, according to an equilibrium curve, until a certain temperature.

The experiments are carried out injecting methanol drop from the bottom side of the test cell and the cell is filled by cyclohexane. The drop is locked to its initial position and anchored to the position of the needle (or capillary tube) used to inject the liquid into the matrix.

The liquids are assumed with constant phase density and transport coefficients. The drop is bounded by a spherical liquid/liquid interface whose radius changes in time due to growth or dissolution.

The hypothesis of spherical surface is acceptable if zero-g conditions prevail or, on the ground, if the volume of the liquid drop is small (few millimetres) and/or if the density difference between the two phases is very low.

Moving boundary method

In the present paragraph, ancient 'moving boundary' numerical methods and in particular possible novel strategies are briefly outlined in order to point out analogies, similarities and difference with the sophisticated numerical algorithm proposed here for the case of growth or dissolution of drops in matrices of different liquids (DDVOF-Dissolution of drops Volume of Fraction Method).

The numerical simulations of these problems require a discretization or nodalization to allow numerical treatment on computers. There are two fundamentally different approaches: Eulerian methods use a frame of reference (discretization grid or mesh, control volumes, etc.) fixed in space, and matter moving through this frame of reference. Lagrangian methods instead use a frame of reference (marker particles) fixed to and moving with the matter.

The first method capable of modelling multi-phase flow, separated by a moving interface, was the Marker and Cell (MAC) of Harlow and Welch [7]. This was in fact a combination of an Eulerian solution of the basic flow field, with Lagrangian marker particles attached to one phase to distinguish it from the other phase. While the staggered mesh layout and other features of MAC have become a model for many other Eulerian codes, the marker particles proved to be computationally too expensive and have been rarely used.

In the specific case of drops growing or dissolving in a matrix of different liquid and in order to introduce novel numerical techniques, one must generally accomplish at least two things simultaneously: (a) determine the concentration fields in both the liquid phases and (b) determine the position of the interface between the phase 1 and the phase 2. According to the technique used

to address (a) and (b), in principle the numerical procedures able to solve these problems can be divided into two groups:

1) Multiple region solutions utilizing independent equations for each phase and coupling them with appropriate boundary conditions at the interface. This approach to the problem takes the point of view that the interface separating the bulk phases is a mathematical boundary of zero thickness where interfacial conditions are applied. These interfacial conditions couple to the concentration equations in the bulk and this system of equations and boundary conditions provides a means to address (a) and (b). Difficulties arise when this technique is employed since in this case in the vicinity of the interface, conditions on mass flux, velocity, and solubility evolution have to be accounted for. This effectively rules out the application of a fixed-grid numerical solution, as deforming grids or transformed co-ordinate systems are required to account for the position of the phase front.

2) Single region (continuum) formulations (or 'phase field' models) which eliminate the need for separate equations in each phase, by establishing conservation equations which are universally valid. From a theoretical point of view the major advantage of the single region formulations is that they do not require the use of quasi-steady approximations, numerical remeshing and co-ordinate mapping.

In a phase-field model, a phase-field variable ϕ which varies in space and time is introduced to characterize the phase. In place of the 'sharp' transition from one phase to the other that would characterize the multiple region formulations, here the phase-field varies smoothly but rapidly through an interfacial region. The effect is a formulation of the free boundary problem that in principle does not require application of interfacial conditions at the unknown location of a phase boundary. This formulation is at the base of the most recent and popular methods used for moving boundary problems (Volume of fluid VOF methods, see e.g. Hirt et al. [8], Osher et al. [9], Gueyffier et al. [10]; enthalpy methods, see e.g. Bennon and Incropera [11,12], Voller and Prakash [13]). For this reason in the present paper this strategy is adopted.

DDVOF - Volume of Fraction Method for dissolving drops.

The DDVOF is a single region formulation and allows a fixed-grid solution to be undertaken. It is therefore able to utilize standard solution procedures for the fluid flow and species equations directly, without resorting to mathematical manipulations and transformations.

The model is based on the mass balance equations. The diffusion of the species is governed by the equations (drop=phase 1→ϕ=1, matrix=phase 2→ϕ=0):

$$\frac{\partial C_1}{\partial t} = \phi\left[-\underline{\nabla}\cdot\left(\underline{V}C_1\right) + D\ \nabla^2 C_1\right] \qquad (1)$$

$$\frac{\partial C_2}{\partial t} = (1-\phi)\left[-\underline{\nabla}\cdot\left(\underline{V}C_2\right) + D\ \nabla^2 C_2\right] \qquad (2)$$

Where D is the interdiffusion coefficient.

The species equations (1) and (2) are solved throughout the computational domain including the drop and the matrix. The presence of the terms ϕ and (1-ϕ) ensures in fact that each equation characterizes a different phase. At the initial instant both the phases are supposed to be at constant concentration ($C_{1(o)}$ and $C_{2(o)}$ respectively).

The behaviour of the two phases is coupled through the equilibrium concentration values imposed on the two sides of the interface. These values come from the miscibility law (see Fig. 5). On the interface (0<ϕ<1), the concentrations must satisfy the equilibrium conditions:

$$C_1\big|_i = C_{1(e)} \qquad (3)$$

$$C_2\big|_i = C_{2(e)} \qquad (4)$$

Equations (3), and (4) behave as 'moving boundary conditions'. Note that in place of the 'sharp' transition from one phase to the other that would characterize the multiple region formulations (in that case the interface separating the bulk phases is a mathematical boundary of zero thickness), here the phase-field varies smoothly but rapidly through an interfacial region whose thickness is not zero. This region, defined by the mathematical conditions $\left|\underline{\nabla}\phi\right| \neq 0$,0<ϕ<1, moves through the

computational domain according to the behaviour of the different phases (i.e. according to the behaviour of ϕ).

The flow is governed by the continuity, and Navier-Stokes equations:

$$\underline{\nabla} \cdot \underline{V} = 0 \tag{5}$$

$$\frac{\partial(\rho \underline{V})}{\partial t} = -\underline{\nabla} p - \underline{\nabla} \cdot [\rho \underline{V}\underline{V}] + \underline{\nabla} \cdot [\mu \underline{\nabla V}] + \underline{F}_g \tag{6}$$

where

$$\rho = \rho_{1(o)}\phi + \rho_{2(o)}(1-\phi) \tag{7a}$$

$$\mu = \mu_1 \phi + \mu_2 (1-\phi) \tag{7b}$$

and in the last term of equation (6):

$$F_g = g[\beta_1 (C_1 - C_{1(o)})]\phi + g[\beta_2 (C_2 - C_{2(o)})](1-\phi) \tag{7c}$$

the Boussinesque approximation is used to model the buoyancy forces, β_1 and β_2 are the solutal expansion coefficients related to the mutual interpenetration of the phases (1) and (2).

The core of the DDVOF method is its technique for adjourning ϕ. The tracking of the interface between the phases is accomplished by the solution of a special continuity integral equation for the volume of the liquid drop taking into account the release or absorption of solute through the interface. The liquid drop is assumed to be a sphere of radius R increasing due to growth or decreasing due to dissolution. Using mass balance, one obtains for the time evolution of the radius :

$$\frac{dR}{dt} = \frac{D}{C_1|_i - C_2|_i} \frac{1}{S} \oint \left(\frac{\partial C_2}{\partial n}\bigg|_i + \frac{\partial C_1}{\partial n}\bigg|_i \right) dl \tag{8}$$

where S is the surface of the drop,

$$\frac{\partial C}{\partial n} = \underline{\nabla} C \cdot \underline{\hat{n}} = \alpha \frac{\partial C}{\partial x} + \beta \frac{\partial C}{\partial y} \tag{9}$$

$$\underline{\hat{n}} = -\frac{\underline{\nabla}\phi}{|\underline{\nabla}\phi|} = (\alpha, \beta) \tag{10a}$$

$$\alpha = -\frac{\partial \hat{\phi}}{\partial x} \Big/ \sqrt{\left(\frac{\partial \hat{\phi}}{\partial x}\right)^2 + \left(\frac{\partial \hat{\phi}}{\partial y}\right)^2} \qquad (11a)$$

$$\beta = -\frac{\partial \hat{\phi}}{\partial y} \Big/ \sqrt{\left(\frac{\partial \hat{\phi}}{\partial x}\right)^2 + \left(\frac{\partial \hat{\phi}}{\partial y}\right)^2} \qquad (11b)$$

The unit vector $\underline{\hat{n}}$ perpendicular to the interface results from the gradient of a smoothed phase field $\hat{\phi}$, where the transition from one phase to the other takes place continuously over several cells (typically 4 or 5 for a grid having 200x200 points). The smoothed phase field $\hat{\phi}$ is obtained by convolution of the unsmoothed field ϕ with an interpolation function. The interface orientation depends on the direction of the volume fraction gradient of the phase $\hat{\phi}$ within the cell, and that of the neighbour cell (or cells) sharing the face in question. Depending on the interface's orientation and on the side (phase (1) or phase (2)) on which computations are performed, concentration gradients are discretized by forward or backward schemes.

Equations (12):

$|\underline{\nabla\phi}| \neq 0$, $\alpha>0$, $\beta>0$ $\quad \frac{\partial C_1}{\partial n} = \left(-\alpha\ C_{1i-1,j} / \Delta x - \beta\ C_{1i,j-1} / \Delta y\right) - C_{1i,j}\left(-\alpha / \Delta x - \beta / \Delta y\right)$

$|\underline{\nabla\phi}| \neq 0$, $\alpha<0$, $\beta>0$ $\quad \frac{\partial C_1}{\partial n} = \left(\alpha\ C_{1i+1,j} / \Delta x - \beta\ C_{1i,j-1} / \Delta y\right) - C_{1i,j}\left(\alpha / \Delta x - \beta / \Delta y\right)$

$|\underline{\nabla\phi}| \neq 0$, $\alpha>0$, $\beta<0$ $\quad \frac{\partial C_1}{\partial n} = \left(-\alpha\ C_{1i-1,j} / \Delta x + \beta\ C_{1i,j+1} / \Delta y\right) - C_{1i,j}\left(-\alpha / \Delta x + \beta / \Delta y\right)$

$|\underline{\nabla\phi}| \neq 0$, $\alpha<0$, $\beta<0$ $\quad \frac{\partial C_1}{\partial n} = \left(\alpha\ C_{1i+1,j} / \Delta x + \beta\ C_{1i,j+1} / \Delta y\right) - C_{1i,j}\left(\alpha / \Delta x + \beta / \Delta y\right)$

Equations (13):

$|\underline{\nabla\phi}| \neq 0$, $\alpha>0$, $\beta>0$ $\quad \frac{\partial C_2}{\partial n} = \left(\alpha\ C_{2i+1,j} / \Delta x + \beta\ C_{2i,j+1} / \Delta y\right) - C_{2i,j}\left(\alpha / \Delta x + \beta / \Delta y\right)$

$|\underline{\nabla\phi}| \neq 0$, $\alpha<0$, $\beta>0$ $\quad \frac{\partial C_2}{\partial n} = \left(-\alpha\ C_{2i-1,j} / \Delta x + \beta\ C_{2i,j+1} / \Delta y\right) - C_{2i,j}\left(-\alpha / \Delta x + \beta / \Delta y\right)$

$|\underline{\nabla\phi}| \neq 0$, $\alpha>0$, $\beta<0$ $\quad \frac{\partial C_2}{\partial n} = \left(\alpha\ C_{2i+1,j} / \Delta x - \beta\ C_{2i,j-1} / \Delta y\right) - C_{2i,j}\left(\alpha / \Delta x - \beta / \Delta y\right)$

$|\underline{\nabla\phi}| \neq 0$, $\alpha<0$, $\beta<0$ $\quad \frac{\partial C_2}{\partial n} = \left(-\alpha\ C_{2i-1,j} / \Delta x - \beta\ C_{2i,j-1} / \Delta y\right) - C_{2i,j}\left(-\alpha / \Delta x - \beta / \Delta y\right)$

Then the distribution of the phase variable ϕ is defined according to the radius of the drop at the new instant (n+1):

$r<R$, $\phi=1$ (14a)

$r>R$, $\phi=0$ (14b)

Equations (1), (2), (5), (6) and (8) represent a system of four partial differential equations and one ordinary differential equation whose solution governs the non-linear behaviour of the physical system under investigation.

Note that the present mathematical model and related numerical technique can be seen as a very hybrid volume of fluid method.

In the "classical" VOF methods, the phase field variable ϕ is ‘advected’ solving an appropriate partial differential transport equation; this formulation has been often used for the solution of typical problems dealing with the migration of bubbles or drops posed in liquids. It relies on the fact that the fluids are not interpenetrating. For the present method the equation governing the evolution of ϕ comes from mass balance conditions rather than from transport. Moreover interpenetration of the different fluids is allowed according to the coupled behaviour of equations (1), (2) and (8).

Equation (8) moreover provides the necessary coupling among the species and momentum equations. The density and the dynamic viscosity of the liquid in eq. (6) in fact are computed according to the instantaneous distribution of ϕ. Further coupling between the species and momentum equations is due to the volume force term (Boussinesque approximation) in eq. (6).

Discretization and solution

Eqs. (1,2,5,6) subjected to the initial and boundary conditions are solved numerically in primitive variables by a control volume method. The domain is discretized with a cylindrical axisymmetric uniform mesh and the flow field variables defined over a staggered grid. Forward differences in time and upwind schemes in space (second order accurate) are used to discretize the partial differential equations

The computation of the velocity field at each time step is split into two substeps.

In the first, an approximate non-solenoidal velocity field $\underline{V}^*$ which corresponds to the correct vorticity of the field is computed at time (n+1) neglecting the pressure gradient term in the momentum eq. (6). In the second substep, the pressure field is computed by solving the equation resulting from the divergence of the momentum equation taking into account eq. (5):

$$\nabla^2 p_k = \frac{1}{\Delta t} \underline{\nabla} \cdot \underline{V}_k^* \qquad k=1,2 \qquad (15)$$

This equation is solved with a SOR (Successive Over Relaxation) iterative method. For further details on the numerical method see e.g. Monti, Savino, Lappa and Tempesta [14], Lappa [15], Lappa and Savino [16]. On the solid walls the $\partial P/\partial n=0$ condition is imposed; at the interface, this condition is discretized by forward or backward schemes according to the interface's orientation and to the phase :

Phase (1)=drop

$0<\phi<1,\ \alpha>0,\ \beta>0 \qquad P_{i,j} = \dfrac{\left(-\alpha\ P_{i-1,j}/\Delta x - \beta\ P_{i,j-1}/\Delta y\right)}{\left(-\alpha/\Delta x - \beta/\Delta y\right)}$ (16a)

$0<\phi<1,\ \alpha<0,\ \beta>0 \qquad P_{i,j} = \dfrac{\left(\alpha\ P_{i+1,j}/\Delta x - \beta\ P_{i,j-1}/\Delta y\right)}{\left(\alpha/\Delta x - \beta/\Delta y\right)}$ (16b)

$0<\phi<1,\ \alpha>0,\ \beta<0 \qquad P_{i,j} = \dfrac{\left(-\alpha\ P_{i-1,j}/\Delta x + \beta\ P_{i,j+1}/\Delta y\right)}{\left(-\alpha/\Delta x + \beta/\Delta y\right)}$ (16c)

$0<\phi<1,\ \alpha<0,\ \beta<0 \qquad P_{i,j} = \dfrac{\left(\alpha\ P_{i+1,j}/\Delta x + \beta\ P_{i,j+1}/\Delta y\right)}{\left(\alpha/\Delta x + \beta/\Delta y\right)}$ (16d)

Phase (2)=matrix

$0<\phi<1,\ \alpha>0,\ \beta>0 \qquad P_{i,j} = \dfrac{\left(\alpha\ P_{i+1,j}/\Delta x + \beta\ P_{i,j+1}/\Delta y\right)}{\left(\alpha/\Delta x + \beta/\Delta y\right)}$ (17a)

$0<\phi<1,\ \alpha<0,\ \beta>0 \qquad P_{i,j} = \dfrac{\left(-\alpha\ P_{i-1,j}/\Delta x + \beta\ P_{i,j+1}/\Delta y\right)}{\left(-\alpha/\Delta x + \beta/\Delta y\right)}$ (17b)

$0<\phi<1,\ \alpha>0,\ \beta<0 \qquad P_{i,j} = \dfrac{\left(\alpha\ P_{i+1,j}/\Delta x - \beta\ P_{i,j-1}/\Delta y\right)}{\left(\alpha/\Delta x - \beta/\Delta y\right)}$ (17c)

$0<\phi<1,\ \alpha<0,\ \beta<0 \qquad P_{i,j} = \dfrac{\left(-\alpha\ P_{i-1,j}/\Delta x - \beta\ P_{i,j-1}/\Delta y\right)}{\left(-\alpha/\Delta x - \beta/\Delta y\right)}$ (17d)

Finally, the correct solenoidal velocity field is updated using the computed pressure field to account for continuity:

$$\underline{V}^{n+1} = \underline{V}^{*} - \Delta t \underline{\nabla}\ p^{n} \qquad (18)$$

RESULTS AND DISCUSSION

Figure 8 shows the computed evolution of the concentration and flow field patterns at the beginning of the dissolution process. The numerical results refer to a droplet of Methanol dissolving into a

matrix of Cyclohexane at ambient temperature. The initial volume of the droplet is 3 [μl]. The computations are carried out considering normal (Earth) gravity and therefore buoyancy effects. The results of Figure 8 show the streamlines and the concentration of Methanol around the dissolving droplet at different times. The plume starts rising and after t=100 seconds a fully developed velocity and concentration field is established.

Figure 6 shows the computed time dependence of the average drop radius. The initial volume of the drop is the same as in Figure 8 (3 [μl]). The numerical simulations have been carried out in the two cases: a) zero gravity conditions (i.e. zero buoyancy); b) Earth gravity conditions (i.e. in the presence of buoyancy convection). The numerical results show that buoyancy induced convection increases the drop dissolution, in comparsion with the purely diffusive situation. The volume of the drop decreases more rapidly as time increases, and better correlation with the experimental results is achieved if convection is taken into account.

As discussed in Section 2, the experiments performed with binary liquid-liquid systems have shown that the phenomena under investigation may exhibit "stable" rising solutal plumes (created above the dissoving drop) or "pulsating" jets showing time-dependent oscillatory behaviour.

For sufficiently small values of the initial volume of the drop, the convection in the liquid column is laminar and steady, but if this initial volume exceeds certain critical values depending on the binary liquid-liquid system and on the temperature, the liquid motion can undergo a transition to an oscillatory axisymmetric complex flow pattern.

Note that the experimental fringes around the dissolving drop describe in the observation plane well defined curves whose shape approximately looks like two symmetric folds disposed on the left and right sides of the drop (see Figure 7). The pulsating behaviour consists in a "periodic" expansion and contraction of the two folds. The velocity and the concentration fields are symmetric and the time-dependence is observed as a synchronous pulsation of these symmetrical folds (they travel axially up and down). The periodic motion is not confined however to the zone close to the drop surface and affects also the behaviour of the rising ject carrying methanol towards the top of the

test cell. The instability in fact leads somehow to a "periodic release" of a "packet" of lighter fluid in the plume. This phenomenon appears in the form of a periodic expansion of the diameter of the rising jet. This expansion behaves as a disturbance travelling towards the top (i.e. a perturbation of the solutal and flow field rising along the core of the plume).

These behaviours have been confirmed by the numerical simulations (Figs. 9 and Figs.10). The mathematical model and the associated numerical algorithm have proven to be able to "capture" the complex time-dependent phenomena and to provide information and data about the intrinsic nature of the instability. Computations obtained "switching off" surface tension effects, in fact have proved that the phenomena under investigation are driven by the buoyancy (gravitational) effect whereas the solutal Marangoni flow does not seem to play a critical role in the onset of the flow instability.

Figs. 8 (numerical computations) show the presence of a large toroidal convection roll wrapped around the solutal jet. The instability is hydrodynamic in nature, i.e. it does not depend on the behaviour of the solutal field (for this instability the solutal field simply acts as a "driving force" for the velocity field). When the velocity of the particles exceed a certain critical value, bifurcation to oscillatory flow occurs. This explains why the instability occurs only if a certain initial value of the drop volume is exceeded whereas the flow exhibits stable solutal rising plumes in the case of small initial volumes; the maximum velocity in the core of the rising plume in fact depends on the flow rate of methanol through the drop interface; in turn this flow rate depends on the surface area of the drop and therefore on its radius (i.e. volume).

With regard the nature of the instability, note that the phenomena here discussed exhibit surprising analogies with behaviours previously observed in the case of different phenomena (see Cetegen and Ahmed [17], Cetegen and Kasper [18], Cetegen [19], Cetegen et al. [20]).

Cetegen [19] carried out experimental studies dealing with the instabilities and flow transitions of buoyant plume/jets of gas mixtures. The author investigated the case of a buoyant plume of helium or helium/air mixture originating from a large axisymmetric nozzle with low velocity. He found

toroidal vortex formation as a result of rapid buoyant acceleration of light plume fluid in heavier more or less quiescient surroundings.

It was found that these plumes may undergo periodic oscillations with a macroscopic behaviour very similar to that described in the present paper: as the buoyant fluid exits the nozzle, plume boundary contracts towards the plume centerline as a result of buoyant acceleration due to the hydrostatic pressure field and the condition imposed by the conservation of mass; the plumes undergo periodic oscillations of the plume boundary starting in the immediate vicinity of the nozzle lip. This behaviour strongly resembles that observed in the present study about the periodic pulsation of the two folds close to the drop surface.

Moreover, in analogy with the present case of solutal plumes, it was found experimentally by Cetegen [19] that not all buoyant plumes exhibit periodic oscillations. The onset of oscillations is, in general, a function of nozzle diameter, nozzle exit velocity and the density ratio between the plume fluid and its surrounding (Cetegen [19]) as for the present case, instability occurs only if a critical initial volume of the drop is exceeded.

Cetegen and Kasper [18] provided a very inteersting explanation of these phenomena: the mechanism leading to the periodic oscillatory state of the flow field is connected with the highly unstable (Rayleigh-Taylor) density stratification in the sharply contracting region of the flow just above the nozzle exit. According to the numerical simulations. the same mechanism applies to the present case of solutal flow where unstable density stratification occurs just above the dissolving drop.

Note that important analogies can be found also about the behaviour of "pool fires". It is well known (Cetegen and Ahmed, [17]) that axisymmetric pool fires exhibit a periodic oscillatory motion close to their origin, often referred to as "puffing". In a fire, these periodic oscillations result in formation of large-scale (of the order of burner diameter) flaming vortical structures at a short distance from the burner surface. These structures significantly modify the downstream flame behaviour as they rise through the flame and finally burnout near the flame top.

Again the behaviour is very similar to that observed in the case of the periodic "release" of packets of fluid in the rising jet generated above the dissolving drop. The perturbation in the solutal jet diameter originated at the drop surface rises along the core of the jet and dies at the top.

In summary, the presence of puffing in isothermal helium plumes, in flames and in the phenomena associated to the dissolution of drops in liquids exhibiting a miscibility gap, suggests that the puffing phenomenon is associated with the instability of the buoyant flow.

In the case of helium plumes the force driving the instability is the pressure gradient between the helium reservoir and the ambient. In the case of flames and fires, the driving force is the release of heat in the core of the flame due to the combustion process; puffing in pool fires in fact is typically stronger than buoyant nonreacting plumes due to the local heat release and the consequently mantained buoyancy. In the present case of solutall plume, the force driving the instability is the dissolution of the drop located on the bottom of the test cell; the dissolution in fact provides continuosly lighter fluid that is carried up due to the buoyancy forces.

ACKNOWLEDGEMENTS

The authors would like to thank Mr. Nicola di Francescantonio for the experiments performed in the frame of his thesis in Aerospace Engineering.

REFERENCES

[1] “Decomposition, Phase separation, Solidification of immiscible liquid alloys”, in *Immiscible liquid metals and organics*, Proceedings of an international workshop organized by the ESA expert working group, "Immiscible alloys" held in the Physikzentrum, Bad Honnef 1992, edited by L. Ratke,Germany, 1992, pp.3-34.

[2] B. Prinz, A. Romero, ”New Casting Process for Hypermonotectic Alloys” , in *Immiscible liquid metals and organics*, Proceedings of an international workshop organized by the ESA expert

working group, "Immiscible alloys" held in the Physikzentrum, Bad Honnef 1992, edited by L. Ratke, Germany, 1992, pp. 281-289.

[3] N.O.Young, J.S. Goldstein, M.J. Block “The motion of bubbles in a vertical temperature gradient”, J. Fluid Mech, **6**, pp. 350-360, (1959).

[4] D. Agble, M.A. Mendes Tatsis: “The effect of surfactants on interfacial mass transfer in binary liquid-liquid systems”, Int. J. Heat and Mass Transfer, **43**, pp. 1025-1034, (2000).

[5] "The Physical-Chemical constants of binary systems", Interscience, New York, (1959).

[6] E. Susana Perez de Ortiz, H. Sawistoski, “Interfacial Instability of binary liquid-liquid systems, I. Stability Analysis, J. Chemical Engineering Science, **28**, pp. 2051-2061, (1973).

[7] F.H. Harlow, J.E. Welch, ‘Numerical calculation of time-dependent viscous incompressible flow with free surface”, Phys. Fluids, **8**, pp. 2182-2189, (1965).

[8] C.W. Hirt, B.D. Nichols, ‘Volume of Fluid (VOF) Method for the Dynamics of Free Boundaries’, J. Comput. Phys., **39**, pp. 201-225, (1981).

[9] S.Osher, J.A.Sethian, ‘Fronts propagating with curvature-dependent speed: Algorithms based on Hamilton-Jacobi formulations’, J. Comput. Phys., **79**, pp. 12-49 , (1988).

[10] D. Gueyffier, J. Li, A. Nadim, S. Scardovelli, S. Zaleski, ‘Volume of Fluid interface tracking with smoothed surface stress methods for three-dimensional flows’, J. Comput. Phys., **152**, pp. 423-456, (1999)

[11] W.D. Bennon, F.P. Incropera, ‘A continuum model for momentum, heat and species transport in binary solid-liquid phase change systems-I. Model formulation’, Int.J.Heat Mass Transfer, **30** (10), pp. 2161-2170, (1987).

[12] W.D. Bennon, F.P. Incropera, ‘A continuum model for momentum, heat and species transport in binary solid-liquid phase change systems-II. Application to solidification in a rectangular cavity’, Int.J.Heat Mass Transfer, **30** (10), pp. 2171-2187 (1987).

[13] V. R.Voller, C. Prakash, ‘A fixed grid numerical modelling methodology for convection-diffusion mushy region phase-change problems’, Int. J. Heat Mass Transfer, **30** (8), pp. 1709-1719, (1987).

[14] R. Monti, R. Savino, M. Lappa, S. Tempesta, ‘Behaviour of drops in contact with liquid surfaces at non wetting conditions’**;** Phys. Fluids, **10** (11), pp. 2786-2796 (1998)**.**

[15] M. Lappa M., ‘Strategies for parallelizing the three-dimensional Navier-Stokes equations on the Cray T3E ‘; Science and Supercomputing at CINECA, **11**, pp. 326-340, (1997).

[16] M. Lappa, R. Savino, ‘Parallel solution of three-dimensional Marangoni flow in liquid bridges’, Int. J. Num. Meth. Fluids, **31**, pp. 911-925 (1999).

[17] B.M. Cetegen, T. A. Ahmed,”Experiments on the periodic instability of buoyant plumes and pool fires”, Combustion and flame , **93**, pp. 157-184, (1993).

[18] B.M. Cetegen, K.D. Kasper,”Experiments on the oscillatory behaviour of buoyant plumes of helium and helium-air”, Phys. Fluids, **8** (11) pp.2974-2984, (1996).

[19] B.M. Cetegen,”Behaviour of naturally oscillating and periodically forced axisymmetric buoyant plumes of helium and helium-air mixtures”, Phys. Fluids, **9**, (12), pp. 3742-3753, (1997).

[20] B.M. Cetegen, Y. Dong, C. Soteriou,”Experiments on -stability and oscillatory behaviour of planar buoyant plumes”, Phys. Fluids, **10** (7), pp. 1658-1665, (1998).

List of captions

Figure 1: Sketch of the geometrical configuration

Figure 2. Rising plume from a droplet of Buthanol dissolving in water at ambient temperature (initial drop volume of 1.5 [μl])

Figure 3. Descending flow from a droplet of Methanol dissolving in Hexane at ambient temperature (initial drop volume of 1.5 [μl])

Figure 4. Rising plume from a droplet of Methanol dissolving in Cyclohexane at ambient temperature (initial drop volume of 3 [μl])

Figure 5. Phase diagram (a) and density versus Methanol concentration (b) for the Cycloexane-Methanol system

Figure 6. Time evolution of the measured average drop radius and comparison with numerical results. The initial volume of the droplet (Methanol) is 3 [μl]. The matrix is Cyclohexane.

Figure 7. Oscillatory instability of the axisymmetric plume rising from a drop of Methanol dissolving in a Cyclohexane matrix at ambient temperature. The initial volume of the drop is 5 [μl]. The images are taken at time intervals of 1 seconds.

Figure 8. Computed evolution of the concentration and flow field patterns at the beginning of the dissolution process (droplet of Methanol dissolving into a matrix of Cyclohexane at ambient temperature, initial volume of the droplet 3 [μl], Vmax= 5.4 10^{-2} [cm/s]).

Figure 9. Computed evolution of the unstable solutal plume: concentration and flow field patterns for a 3 [μl] droplet of Methanol dissolving into a matrix of Cyclohexane at ambient temperature (Vmax= 5.4 10^{-2} [cm/s]).

Figure 10. Computed pulsating behaviour close to the surface of the dissolving drop (Figs (a) and (b) refer to the maximum and to the minimum of an oscillation period respectively)

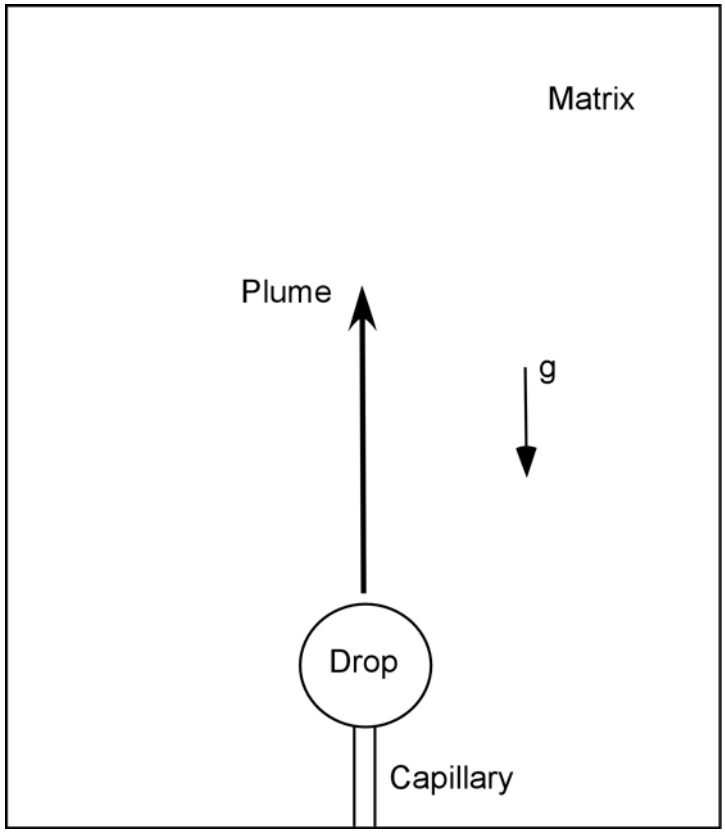

Figure 1: Sketch of the geometrical configuration

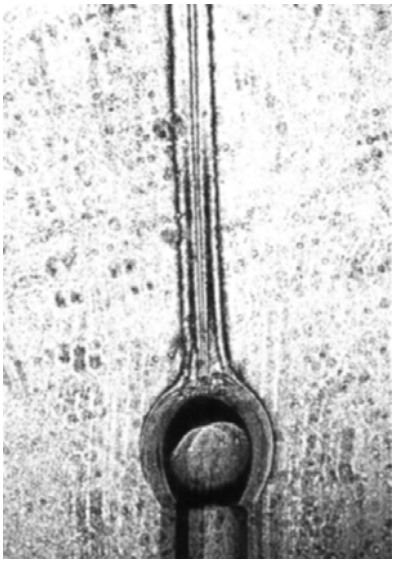

Figure 2. Rising plume from a droplet of Buthanol dissolving in water at ambient temperature (initial drop volume of 1.5 μl)

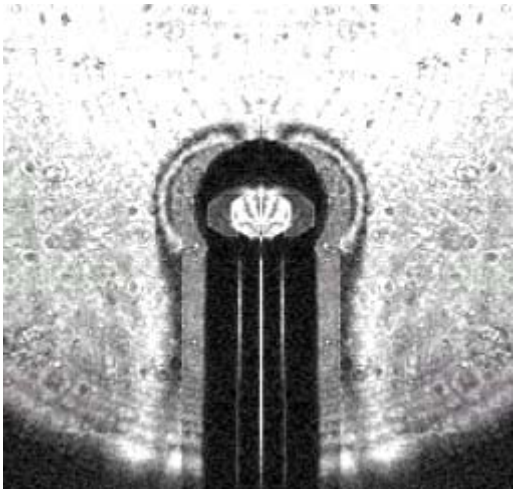

Figure 3. Descending flow from a droplet of Methanol dissolving in Hexane at ambient temperature (initial drop volume of 1.5 μl)

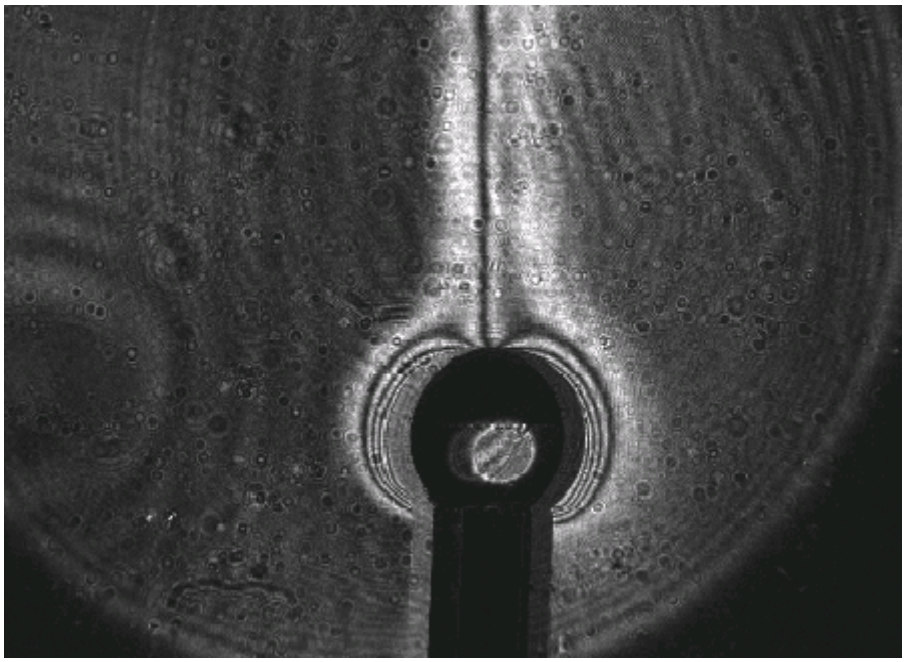

Figure 4. Rising plume from a droplet of Methanol dissolving in Cyclohexane at ambient temperature (initial drop volume of 3 μl)

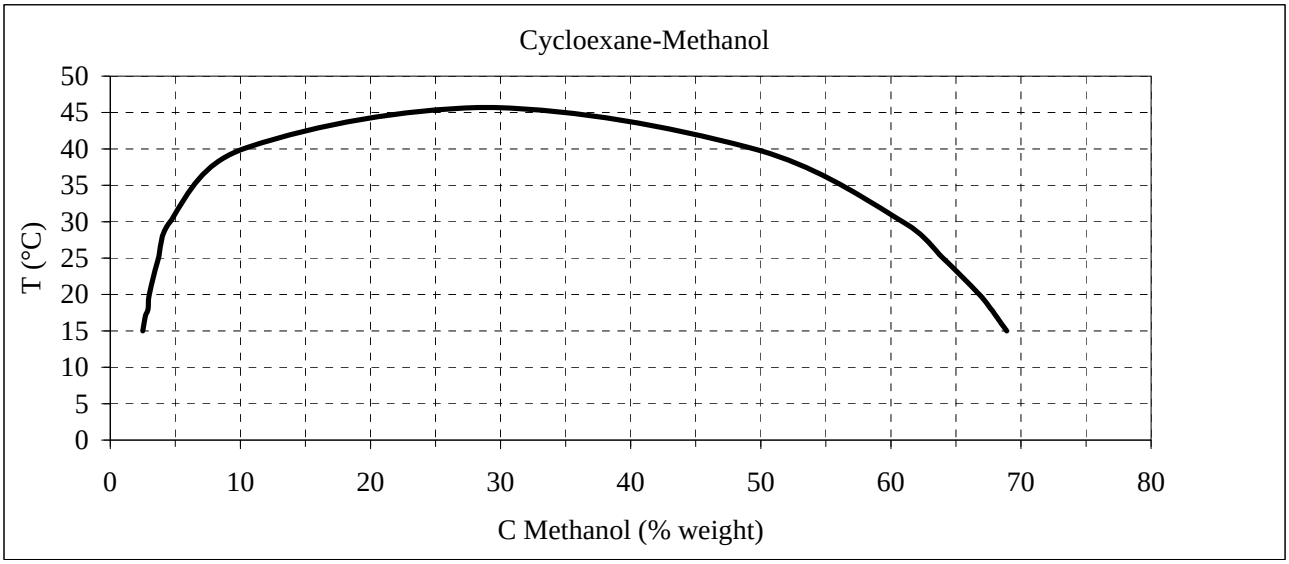

Figure 5. Phase diagram (a) and density versus Methanol concentration (b) for the Cycloexane-Methanol system

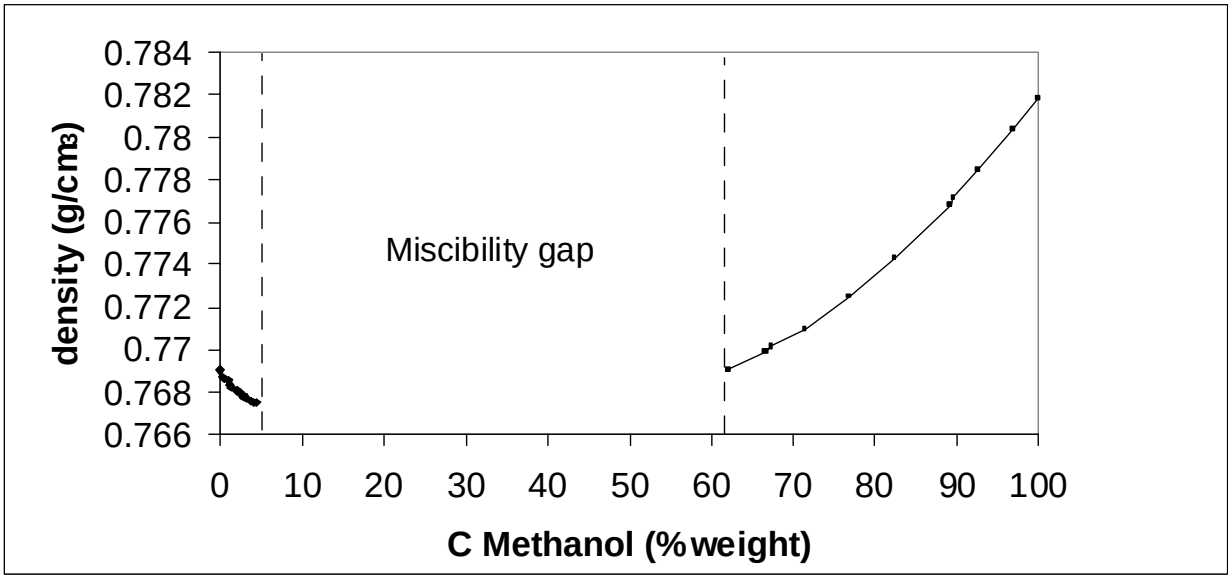

Figure 6. Time evolution of the measured average drop radius and comparison with numerical results. The initial volume of the droplet (Methanol) is 3 [μl]. The matrix is Cyclohexane.

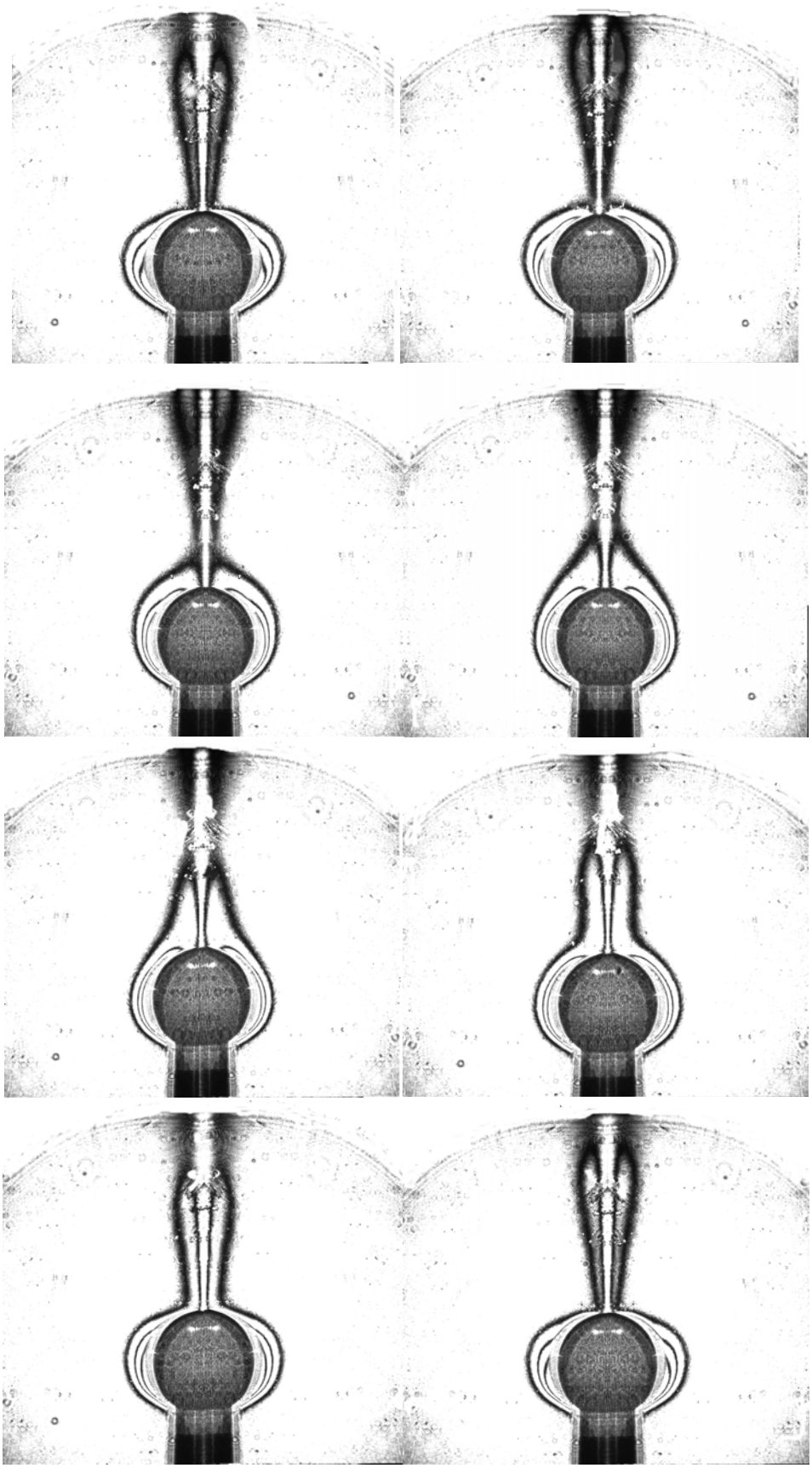

Figure 7. Oscillatory instability of the axisymmetric plume rising from a drop of Methanol dissolvine in a Cyclohexane matrix at ambient temperature. The initial volume of the drop is 5 μl. The images are taken at time intervals of 1 seconds.

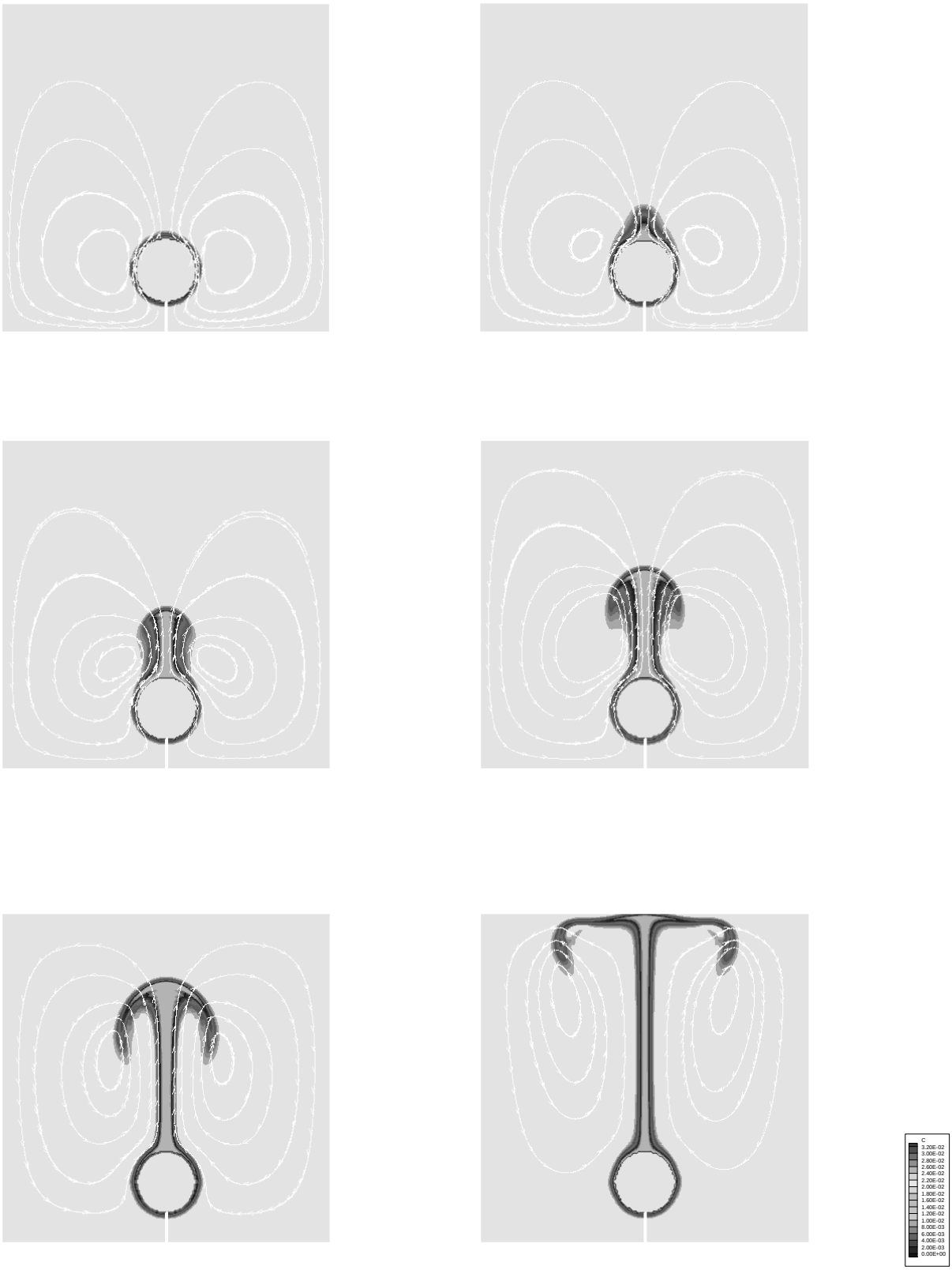

Figure 8. Computed evolution of the concentration and flow field patterns at the beginning of the dissolution process (droplet of Methanol dissolving into a matrix of Cyclohexane at ambient temperature, initial volume of the droplet 3 [μl], Vmax= 5.4 10^{-2} [cm/s]).

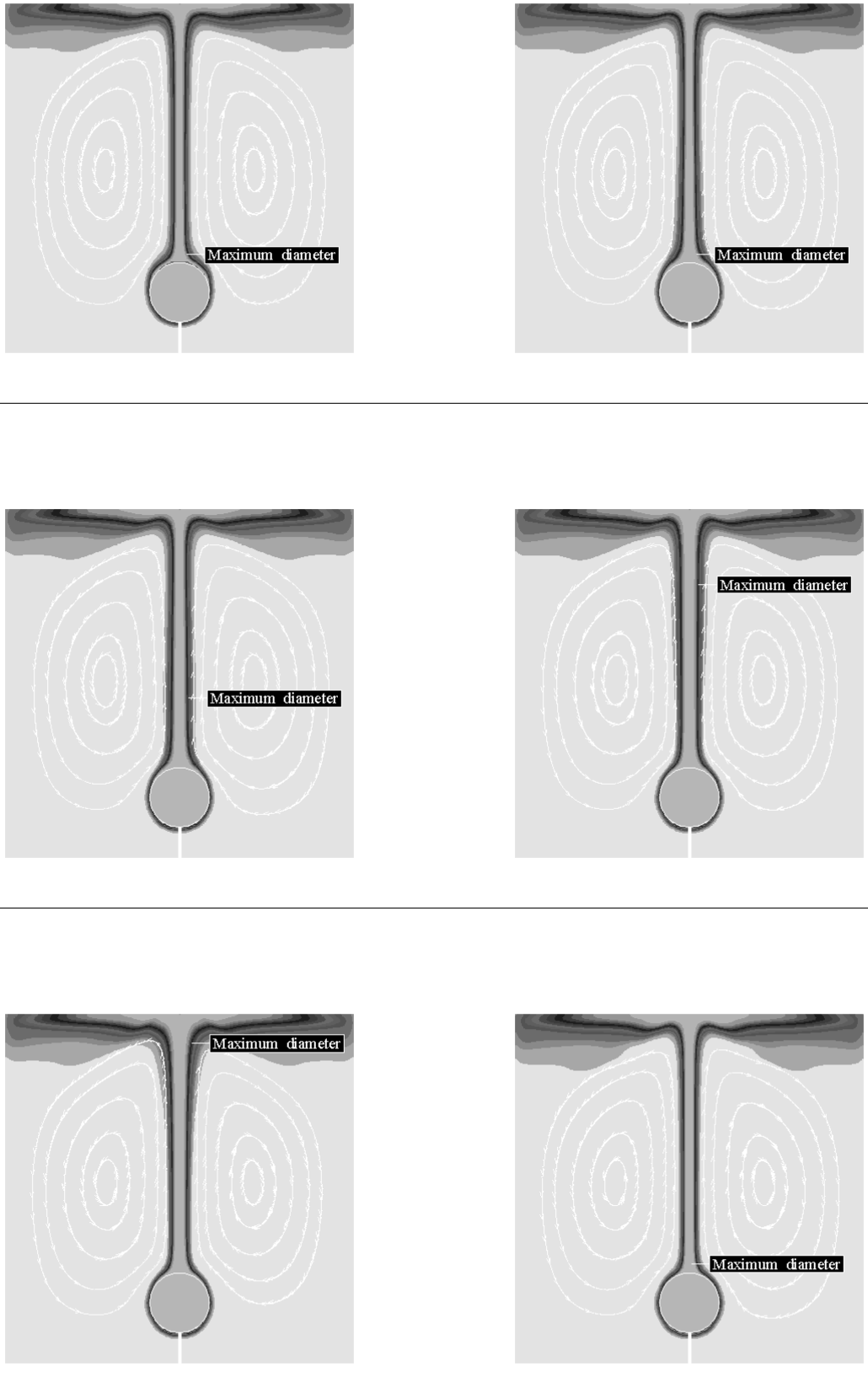

Figure 9. Computed evolution of the unstable solutal plume: concentration and flow field patterns for a 3 [μl] droplet of Methanol dissolving into a matrix of Cyclohexane at ambient temperature (Vmax= 5.4 10^{-2} [cm/s]).

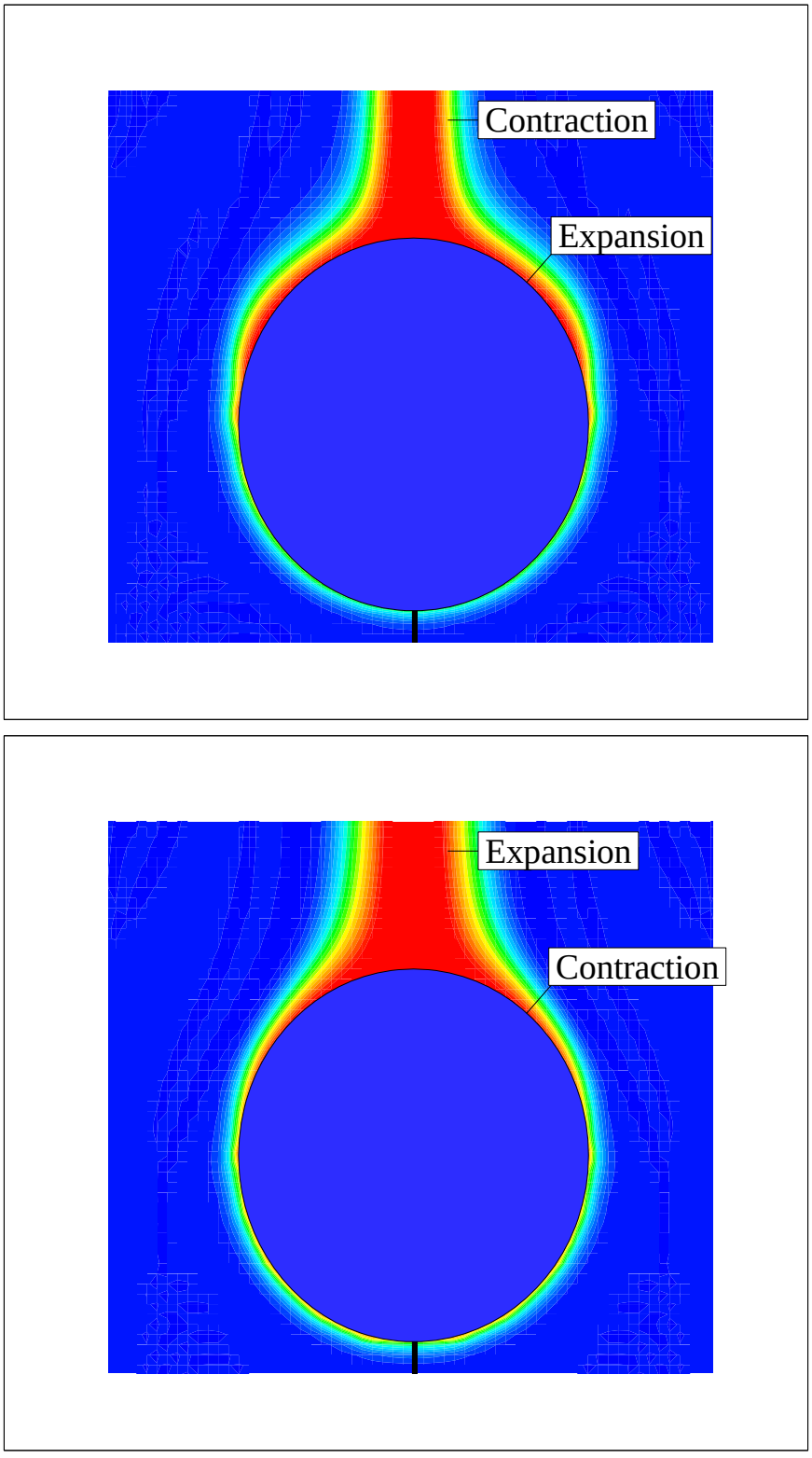

Figure 10. Computed pulsating behaviour close to the surface of the dissolving drop (radial velocity distribution Vmax = 1.5 10^{-2} [cm/s]) (Figs (a) and (b) refer to the maximum and to the minimum of an oscillation period respectively)